Development 137, 1169-1179 (2010) doi:10.1242/dev.045559

Cell death-induced regeneration in wing imaginal discs requires JNK signalling

Cora Bergantiños, Montserrat Corominas and Florenci Serras*

SUMMARY

Regeneration and tissue repair allow damaged or lost body parts to be replaced. After injury or fragmentation of *Drosophila* imaginal discs, regeneration leads to the development of normal adult structures. This process is likely to involve a combination of cell rearrangement and compensatory proliferation. However, the detailed mechanisms underlying these processes are poorly understood. We have established a system to allow temporally restricted induction of cell death in situ. Using Gal4/Gal80 and UAS-*rpr* constructs, targeted ablation of a region of the disc could be performed and regeneration monitored without the requirement for microsurgical manipulation. Using a *ptc-Gal4* construct to drive *rpr* expression in the wing disc resulted in a stripe of dead cells in the anterior compartment flanking the anteroposterior boundary, whereas a *sal-Gal4* driver generated a dead domain that includes both anterior and posterior cells. Under these conditions, regenerated tissues were derived from the damaged compartment, suggesting that compartment restrictions are preserved during regeneration. Our studies reveal that during regeneration the live cells bordering the domain in which cell death was induced first display cytoskeletal reorganisation and apical-to-basal closure of the epithelium. Then, proliferation begins locally in the vicinity of the wound and later more extensively in the affected compartment. Finally, we show that regeneration of genetically ablated tissue requires JNK activity. During cell death-induced regeneration, the JNK pathway is activated at the leading edges of healing tissue and not in the apoptotic cells, and is required for the regulation of healing and regenerative growth.

KEY WORDS: *Drosophila*, Wing disc, Apoptosis, Growth, Regeneration

INTRODUCTION

Over 100 years ago, Morgan (Morgan, 1901) proposed two models to explain animal regeneration: (1) remodelling of existing tissues in the absence of proliferation and (2) local stimulation of cell proliferation. Both mechanisms are known to be used in a variety of organisms, although the extent to which each contributes to the regenerative process in a given tissue is variable (Agata et al., 2007; Chera et al., 2009). In most of the regenerative processes studied to date, a blastema forms near the wound. This involves the generation of a mass of stem cells (Handberg-Thorsager et al., 2008) or precursor cells (Kragl et al., 2009; Lepilina et al., 2006; Poss, 2007) that will grow and contribute to the regenerated tissue. During *Drosophila* larval development, hollow epithelial sacs called imaginal discs give rise to adult structures following metamorphosis. After microsurgical wounding of the imaginal discs, regeneration leads to the development of normal structures (Hadorn et al., 1968). As occurs in amphibian limbs, tadpole tails and zebrafish fins and heart (Brockes and Kumar, 2008; Galliot et al., 2008; Slack et al., 2008), a regeneration blastema forms after cutting a piece of the disc (Bryant, 1971; Bryant and Fraser, 1988; Schubiger, 1971) and, even when isolated, the blastema can regenerate the lost structure (Karpen and Schubiger, 1981). These blastemas display localised proliferation near the wound edges and mitosis and DNA synthesis are observed in the tissue prior to completion of wound healing (Adler, 1981; Bosch et al., 2008; Bryant and Fraser, 1988; Dunne, 1981; Fain and Alvarez, 1987; O'Brochta and Bryant, 1987). However, relatively little is understood about the control of proliferation in these regenerating tissues.

Irradiation of *Drosophila* during larval development can kill up to 40-60% of cells, and yet normal flies still develop through a process of compensatory proliferation (Haynie and Bryant, 1977). One approach to studying the mechanism underlying compensatory proliferation has been to prevent cell death through expression of the baculovirus protein p35 (Hay et al., 1994) following irradiation or induction of apoptosis. Under these conditions, apoptotic cells remain in an 'undead' state (Huh et al., 2004; Perez-Garijo et al., 2004; Ryoo et al., 2004), enabling analysis of the response of cells that remain in contact with them. Such studies have suggested that mitogenic signals, such as Dpp and Wg, are liberated by apoptotic cells (Fan and Bergmann, 2008; Huh et al., 2004; Perez-Garijo et al., 2004; Ryoo et al., 2004) and that caspases can have a non-apoptotic role, functioning as activators of compensatory proliferation (Fan and Bergmann, 2008; Huh et al., 2004). However, other experiments have shown that the downstream effectors of Wg and Dpp are downregulated rather than activated (Wells et al., 2006) and that compensatory proliferation occurs in the absence of Dpp and Wg signals produced by the apoptotic cells (Perez-Garijo et al., 2009). Thus, the signals used to initiate compensatory proliferation remain unclear, or indeed whether they are derived from dying cells or the intact tissue.

JNK signalling has been proposed to mediate the activation of mitogenic factors liberated by 'undead' cells in compensatory proliferation (Ryoo et al., 2004) and hyperplastic disc overgrowth (Perez-Garijo et al., 2009). Furthermore, JNK signalling is activated near the wound in microsurgically ablated imaginal discs, and it has been demonstrated to be required for regeneration in the absence of cell death (Bosch et al., 2008; Bosch et al., 2005; Lee et al., 2005; Mattila et al., 2005). The JNK pathway is also crucial for steering

Departament de Genètica, Facultat de Biologia, and Institut de Biomedicina de la Universitat de Barcelona IBUB, Universitat de Barcelona, Diagonal 645, 08028 Barcelona, Spain.

*Author for correspondence (fserras@ub.edu)

Accepted 31 January 2010

morphogenetic movements in many animal models, including *Drosophila* and mammals. In *Drosophila*, the migrating and spreading properties of the leading edge cells during embryonic dorsal closure (Jasper et al., 2001; Martin and Parkhurst, 2004; Martin and Wood, 2002; Millard and Martin, 2008), disc thorax closure (Agnes et al., 1999; Zeitlinger and Bohmann, 1999) and wound healing after injury (Ramet et al., 2002), as well as in cut and implanted discs during regeneration (Bosch et al., 2005; Mattila et al., 2005), have all been shown to be controlled by this pathway. Wound-healing processes bring together cells from distant positions in the disc following wounding (Bryant and Fraser, 1988) and involve epithelial fusion events (Reinhardt and Bryant, 1981; Reinhardt et al., 1977) and cytoskeletal reorganisation (Bosch et al., 2005). Thus, JNK signalling might be involved in multiple events during the regeneration of *Drosophila* imaginal discs.

Until recently, the analysis of regeneration in *Drosophila* imaginal discs was complicated and involved skilful microsurgery (Bodenstein, 1943; Hadorn, 1963). The sophisticated genetic tools available for use in *Drosophila*, however, raise the possibility of investigating regeneration in situ without the need for mechanical manipulation. For example, a temperature-sensitive cell-autonomous lethal allele of *suppressor of forked* has been used to genetically induce cell death and regeneration in imaginal discs (Brook et al., 1993; Russell et al., 1998). Furthermore, cell death can be locally induced in certain domains of the disc using the Gal4/UAS binary system in combination with *Gal80^{ts}* (Zeidler et al., 2004) to transiently activate pro-apoptotic genes, thereby mimicking microsurgical ablation. This allows cells to be killed in specific domains for a limited time period, after which the tissue recovers and regenerates (Smith-Bolton et al., 2009). In this study, we used a similar genetic approach to activate the apoptotic gene *reaper* (*rpr*) in a temporally and spatially restricted manner, leading to ablation and regeneration of specific domains within the wing disc. Our results show that localised proliferation occurs during the early regeneration events and later extends into the compartment in which cell death was induced. Furthermore, JNK activity is required for the onset of regeneration in the epithelial tissue near the dead domain but is not required in apoptotic cells for normal regeneration to occur.

MATERIALS AND METHODS

Drosophila strains

The *Drosophila* stocks used were *ptc-Gal4* (Hinz et al., 1994), *tub-Gal80^{ts}* (McGuire et al., 2003), *UAS-rpr* (Wing et al., 1998), *Act5c FRT STOP FRT lacZ* (Struhl and Basler, 1993), *puc^{E69}* (Martin-Blanco et al., 1998), *hep^{r75}* (Glise et al., 1995), *spalt^{PE}-Gal4* (Barrio and de Celis, 2004), *salm-Gal4* (provided by J. F. de Celis, Centro de Biología Molecular Severo Ochoa, Madrid, Spain), *UAS-puc2A* (Martin-Blanco et al., 1998), *hh^{ts}* (Ma et al., 1993), *UAS-bsk^{DN}* (Weber et al., 2000), *UAS-Flp* and *UAS-GFP* (Bloomington Stock Center). For the *ptc* domain lineage-tracing experiment (see below) the following genotype was used: *UAS-rpr; ptc-Gal4, UAS-GFP/Act FRT STOP FRT lacZ; UAS-Flp/tub-Gal80^{ts}*. To monitor JNK activity we used the *puc-lacZ* line (*puc^{E69}*) in the following genotype: *ptc-Gal4/tubGal80^{ts}; puc^{E69}/UAS-rpr*.

Cell death induction

To induce cell death in a particular domain of the wing disc at a precise time during development, expression of the pro-apoptotic gene *rpr* (Yoo et al., 2002) was driven using the Gal4/UAS binary system (Brand and Perrimon, 1993) in combination with a temperature-sensitive Gal80 construct to block Gal4 activity (Salmeron et al., 1990). At 17°C, Gal80 is ubiquitously expressed and functional. At 25-29°C, temperature-sensitive Gal80 is inactive (Zeidler et al., 2004), thus relieving the inhibition of Gal4 and activating *rpr* expression. The genotype used was *UAS-rpr; ptc-Gal4 UAS-GFP; tub-Gal80^{ts}*.

Freshly laid eggs were kept at 17°C to prevent *rpr* expression. Larvae were then shifted to 29°C to activate *rpr* for several hours (see Results) and back to 17°C to switch off *rpr* again and allow the tissue to regenerate. It has been reported that full Gal4 activity is not achieved until 6 hours after temperature shift owing to the perdurance of Gal80 (McGuire et al., 2003). We estimated the Gal80 perdurance under our conditions (17°C off, 29°C on) and found that expression of GFP (to label the *ptc* domain) started after 6 hours at 29°C (not shown). Therefore, in all experiments presented here, the temperature shift was performed 6 hours before the timing indicated in the text in order to deplete Gal80 protein.

Developmental times were converted to 25°C equivalents (Ashburner et al., 2005) to facilitate staging (see upper green bar in Fig. 1A). Expression of *rpr* was induced during the third instar larval stage, as depicted in Fig. 1. In some cases in which cell proliferation was studied, *rpr* expression was induced at the end of the third instar (i.e. from 104 to 120 hours after egg laying) in order to minimise basal mitoses. In these experiments, larvae were able to regenerate, although pupation was delayed by ~12 hours.

Adult wings from regenerated and control discs were mounted in lactic acid:ethanol (6:1) and measurements were made of the wing areas and anteroposterior (A/P) and proximodistal axes using ImageJ software (NIH).

Immunostaining and microscopy

Immunostaining was performed using standard protocols. The following primary antibodies were used: anti-Caspase-3 1:1000 (Cell Signaling), anti-phospho-Histone H3 1:1000 (Upstate), anti-GFP 1:1000 (Santa Cruz), anti-BrdU 1:10 (Becton Dickinson), anti-β-galactosidase 1:1000 (Cappel), anti-Ptc 1:50 and anti-En 1:5 (DSHB, University of Iowa), and anti-Ci 1:5 (Motzny and Holmgren, 1995). Fluorescently labelled secondary antibodies were from Molecular Probes and Jackson Immunochemicals. Phalloidin-Rhodamine Red (Invitrogen) was used at 1:20 dilution for 30 minutes after secondary antibody incubation to label the F-actin network. Discs were mounted in Antifade (Molecular Probes, Invitrogen) supplemented with TO-PRO3 1:1000 (Molecular Probes, Invitrogen) to label nuclei.

Images were captured using a Leica SPE confocal microscope and processed and treated with ImageJ and Adobe Photoshop 7.0 software. Some F-actin-labelled images were deconvolved using Huygens Deconvolution Software (Scientific Volume Imaging) and then processed using Imaris software (Bitplane). The number of mitoses was calculated after analysis of stacks of confocal images of *rpr*-induced and control discs using ImageJ (Cell Counter plug-in). Cell number in each area was compared using SPSS software (average comparison test based on Student's *t*-test). Transverse sections were computationally generated after reslicing the confocal stacks using the ImageJ Reslice tool.

BrdU incorporation

For bromo-2′-deoxyuridine (BrdU) incorporation, discs were cultured in Schneider insect medium supplemented with 1 mg/ml BrdU (Sigma-Aldrich) for 10, 20 or 30 minutes. Discs were washed in PBS, fixed in 4% paraformaldehyde and immunostained as described above. Proliferation was also monitored after dilution of incorporated BrdU. Larvae were transferred to yeast-free medium supplemented with a sub-toxic dose of BrdU (1 mg/ml) for 8 hours at 17°C. They were then transferred to standard fly medium at 29°C to induce *rpr* expression. Larvae were finally shifted back to 17°C to stop *rpr* expression and were analysed 36 hours after the BrdU pulse.

TUNEL assay

After fixation of *ptc-Gal4/tubGal80^{ts}; puc^{E69}/UAS-rpr* discs, apoptotic cells were detected using ChromaTide BODIPY FL-14-dUTP (Molecular Probes, Invitrogen) and terminal deoxynucleotidyl transferase (Roche). In the same preparation, primary and secondary antibodies were used to detect *puc-lacZ* expression from the *puc^{E69}* construct.

RESULTS

Experimental design

To induce tissue damage and regeneration, larvae of the *UAS-rpr; ptc-Gal4 UAS-GFP; tub-Gal80^{ts}* genotype grown at 17°C were transferred to 29°C at the appropriate time to activate *rpr* transcription and cell death (Fig. 1A). Use of the *ptc*-Gal4

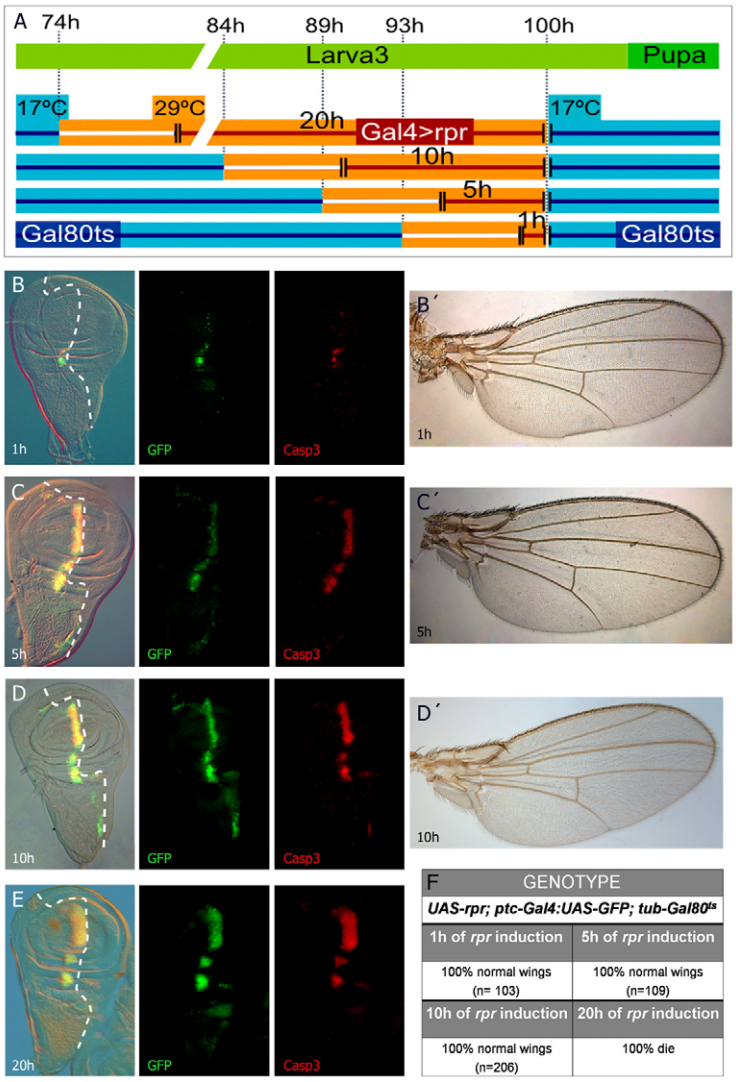

F

GENOTYPE	
UAS-rpr; ptc-Gal4:UAS-GFP; tub-Gal80^{ts}	
1h of *rpr* induction	5h of *rpr* induction
100% normal wings (n= 103)	100% normal wings (n=109)
10h of *rpr* induction	20h of *rpr* induction
100% normal wings (n=206)	100% die

Fig. 1. Regeneration occurs after induction of cell death in *Drosophila* wing discs. (**A**) The cell induction protocol, showing the temperature shifts and the period of exposure (1, 5, 10 and 20 hours) to *rpr*. Blue indicates the period that larvae were kept at 17°C, during which Gal80 binds to Gal4 and inhibits *rpr* expression. Orange indicates the shift to 29°C to induce *rpr* expression. For each time point, an extra 6 hours (white lines in orange bars) were added to deplete Gal80 protein (see main text). Red lines represent *rpr* induction after Gal80 depletion (20, 10, 5 or 1 hour). Green bars represent development through third instar larva (Larva3) up to pupa at 25°C. (**B-E**) *rpr* activation induced for 1, 5, 10 and 20 hours. The left column shows bright-field plus fluorescence, and the middle and right columns show the separate channels of GFP expression in the *ptc* domain (green) and Caspase-3 (red). Regenerated adult wings are shown following development from discs in which cell death was induced for 1 (B′), 5 (C′) and 10 (D′) hours. (**F**) Survival after different times of *rpr* induction.

enhancer led to ablation of a narrow band of anterior cells near the A/P boundary. *UAS-rpr; ptc-Gal4, UAS-GFP; tub-Gal80^{ts}* flies developed normally up to adult stage when kept at 17°C, whereas the genotype was lethal at 25°C. In order to ablate the *ptc* domain in the developing wing and also allow time for regeneration to occur before metamorphosis, *rpr* expression was induced during the mid-third instar larval stage (Fig. 1A). *UAS-rpr; ptc-Gal4, UAS-GFP; tub-Gal80^{ts}* larvae raised at 17°C were shifted to 29°C to induce *rpr* activity for 1, 5, 10 or 20 hours and then brought back to 17°C to stop *rpr* expression. We found that 1, 5 or 10 hours of *rpr* induction (Fig. 1B,C,D) resulted in the regeneration of adult wings that were normal in both size and shape (Fig. 1B′,C′,D′), whereas flies exposed to 20 hours of *rpr* expression died (Fig. 1E,F), probably owing to a failure of other *ptc*-expressing tissues to regenerate following such prolonged apoptosis.

Behaviour of the dead domain

When we examined the extent of cell death, we found that prior to 5 hours of *rpr* induction a small number of activated Caspase-3-positive cells were scattered within the *ptc* domain (see Fig. S1A in the supplementary material). At 5 hours, Caspase-3 staining colocalised with the cell debris, which contained GFP and fragmented nuclei, and accumulated basal to the epithelium (see Fig. S1B in the supplementary material). However, many GFP-expressing cells remained apical and GFP labelling did not colocalise with Caspase-3, suggesting that the *ptc* domain had only been partially eliminated. At 10 hours of *rpr* induction, the Caspase-3-expressing cells formed a broader band with sharply defined edges that separated the dead domain from the living tissue; although most dead cells were concentrated on the basal side, some were still connected to the apical side (see Fig. S1C in the supplementary material). The dead cells accumulated basally and were extruded from the epithelium, as expected based on previous studies (Li and Baker, 2007). Interestingly, few, if any, GFP-positive cells were found on the apical side, suggesting that most of the *ptc* domain had been killed. Hence, we used 10 hours of *rpr* induction for the majority of our analyses.

Behaviour of the regenerating epithelium and cytoskeletal reorganisation

Phalloidin labelling of regenerating discs showed that the columnar epithelium covered the ablated domain (Fig. 2). Initially, cells of the anterior (A) and posterior (P) compartments met at the apical side, whereas the basal part of the epithelium remained open. The most proximal areas of the *ptc* domain were also open and contained dead

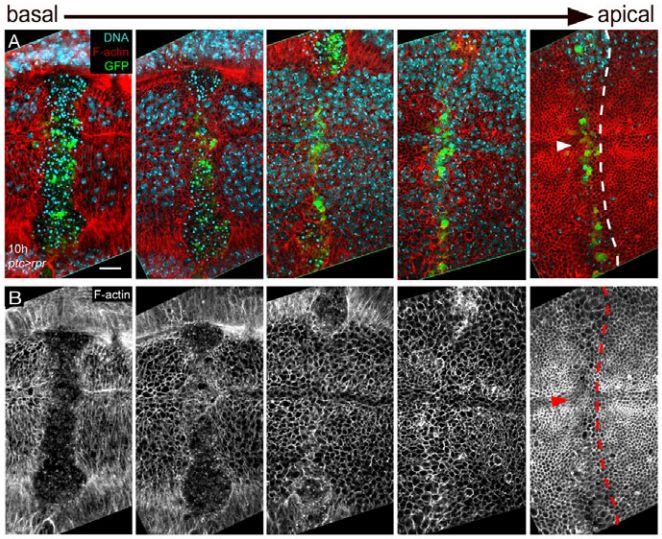

Fig. 2. Confocal sections of phalloidin-labelled wing disc at 10 hours of *rpr* induction. (**A**) Merges of F-actin (red), *ptc*>GFP (green) and nuclei (TO-PRO3, blue). (**B**) Single-channel labelling of F-actin. The healing process can be observed from basal (left) to apical (right). It starts rapidly from the dorsoventral (DV) boundary (arrowhead) and extends progressively to proximal regions until it is almost complete in more apical sections. The anteroposterior (A/P) boundary is indicated with a dashed line. Anterior is to the left and posterior to the right. Scale bar: 15 μm.

cells (Fig. 2). This suggests that apical healing is initiated at the dorsoventral (DV) border and spreads laterally towards proximal regions.

In addition to *ptc*, we also used the *salm-Gal4* driver, which activates Gal4 in the *spalt* (*sal*) domain. The *sal* domain responds to a *dpp* gradient in the central area of the wing pouch and includes cells on either side of the A/P boundary. Our results showed that most of the cells in that domain were ablated after *rpr* induction (see Fig. S2 in the supplementary material) and that healing proceeded from apical to basal and from the DV border to the proximal region, as found for *ptc-Gal4*.

Staining of discs with fluorescently labelled phalloidin immediately after 10 hours of *ptc>rpr* induction revealed that cells at the edges of the wound concentrate F-actin (Fig. 3A). F-actin-rich cell extensions developed along the wound and met other extensions emerging from the other side. These F-actin-rich structures were initially more extended on the apical side of the DV border cells (Fig. 3A,B), where healing was initiated. In addition to these extensions, cells at the edge of the P compartment accumulated F-actin, forming a structure that resembled the F-actin cable described for fragmented discs (Bosch et al., 2005) and during wound repair in embryos (Wood et al., 2002). This F-actin-rich cable was well organised and continuous with the P-compartment edge. By contrast, F-actin accumulation was weaker and discontinuous in cells at the edge of the A compartment (Fig. 3C-C″).

Cell death induced in the *salm-Gal4* domain, which ablates a wider segment of A- and P-compartment cells beyond the A/P boundary, showed similar levels of F-actin accumulation and cell extensions at the edges of the A and P compartments (Fig. 3D,D′) and resembled the F-actin accumulation along the edge of the A compartment in *ptc-Gal4* discs. Because the well-organised F-actin cable in P-compartment leading edge cells was found only after *ptc* domain

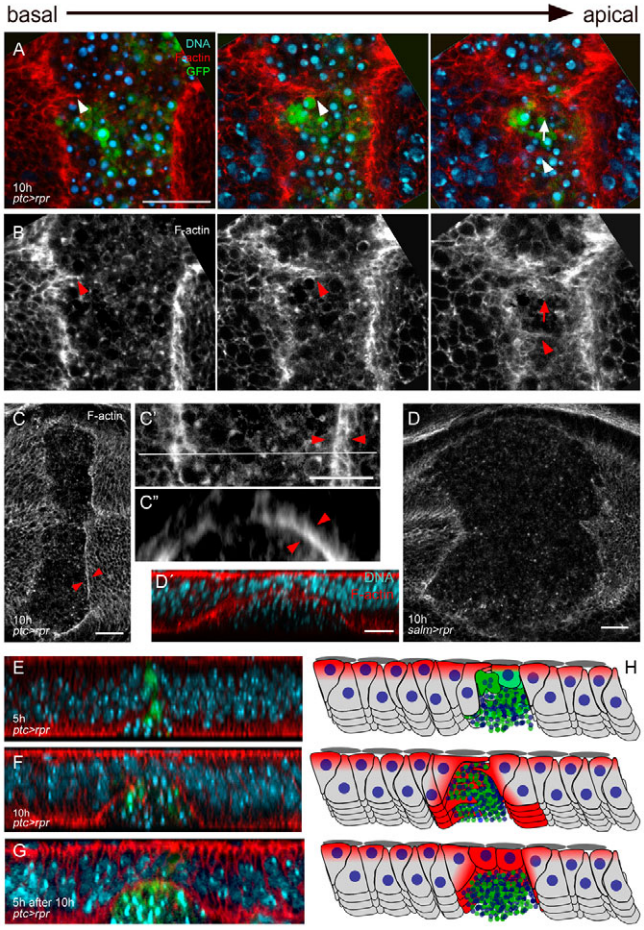

Fig. 3. Cytoskeletal reorganisation during wound repair after *rpr* induction. (**A**,**B**) Three confocal sections of the wound from basal (left) to apical (right) at the level of the DV boundary, showing (A) a merge of GFP from *ptc*-expressing cells (green), nuclei (blue) and F-actin (red), and (B) F-actin alone. In all images, anterior is to the left and posterior to the right. F-actin accumulates at the edges and extended filopodia can be seen in A-compartment cells (arrowhead). In the apical image, F-actin-rich extensions are seen at the A- and P-compartment edges. The arrow points to the DV border, where F-actin-rich extensions first meet. Cellular debris can be seen concentrated in the basal gap. (**C-C″**) Wing disc showing the F-actin-rich cable at the P-compartment edge (arrowheads). (C′) High-magnification view at the level of the arrowheads. Compare the F-actin-rich discontinuous cable at the A-compartment edge with the continuous cable at the P-compartment edge. The thin line in C′ indicates the level of the cross-section through a stack of images (from apical to basal) shown in C″. (**D**) Single basal confocal section of an F-actin-stained wing pouch in which *rpr* has been activated for 10 hours under the *salm* promoter. The dark central zone contains cell debris. (**D′**) Optical section of a disc stack in which *rpr* has been induced with the *salm* promoter. Note that apical healing (top) has been initiated (red, F-actin; blue, nuclei). (**E-G**) Three optical sections through stacks of images showing the apicobasal process of suture when using the *ptc* promoter at the times indicated. Apical is to the top, basal to the bottom. (**H**) Model of healing after induction of cell death. The killed domain (green) removes most cells, and apical extensions rapidly project from the A-compartment edge and later from the P-compartment edge (top). Epithelial extensions projected from both edges meet in the intervening space and pull the epithelium to fill the gap. At the same time, the actin cable keeps the tissue contracted and avoids disorganisation (middle). The pulling together of cells and proliferation refills the domain (bottom). Scale bars: 15 μm.

ablation (Fig. 3C), and not after *salm-Gal4*, it is likely that its function is to prevent the spreading of P cells to the A compartment. In addition, moderate F-actin accumulation might act to promote the meeting of the wound edges, as suggested in other wound-healing events (Jacinto et al., 2002a; Martin and Wood, 2002).

Epithelial integrity was almost recovered 5 hours after *rpr* induction, although cell debris was not yet completely eliminated (Fig. 3E-G). By early pupal stages, integrity was restored, although some debris still remained (not shown). Together, these results point to a model for homotypic healing of the epithelium in which P- and A-compartment edge cells meet apically to initiate epithelial fusion, and the basal membranes progressively pull the epithelium while the actin-rich structures maintain the P- and A-compartment edges (Fig. 3H).

Cell proliferation

On average, 4% of *ptc>GFP* cells survived 10 hours of *rpr* induction, remaining attached to the apical side without entering apoptosis (data from 11 induced discs). To test whether these cells contribute to the reconstruction of the lost domain, cell lineage tracing was carried out with a *lacZ* reporter, which is expressed independently of Gal4. Lineage tracing of *ptc*-expressing cells was analysed 20 hours after the 10 hours of induction [which would correspond to two to three cell cycles during normal development (Garcia-Bellido and Merriam, 1971)]. In control discs lacking *rpr* expression, cells derived from the *ptc* domain were concentrated in the A compartment (Fig. 4A). In *rpr*-induced discs, at least 70% fewer *lacZ*-expressing cells were present, although they continued to be restricted to the A compartment (Fig. 4B,C). This suggests that regeneration of the depleted area is driven by cells from adjacent territories. The proportion of cells derived from the *ptc*-expressing domain might also be underestimated, as some of the *lacZ*-positive cells might correspond to the first derivatives of the *ptc*-expressing domain before death or, alternatively, to the first cells that repopulated the domain and expressed *ptc* in response to Hh signalling from the nearby P compartment.

Analysis of mitosis and BrdU incorporation revealed that both were restricted to the A compartment after *ptc>rpr* induction (see Fig. S3 in the supplementary material). To further explore when and where proliferation was activated in these discs, we performed *ptc>rpr* inductions of 5 hours and 10 hours and then analysed the number of mitotic cells in A and P regions near (A1 and P1) and far (A2 and P2) from the wound (Fig. 5A). There was a significant increase in the number of mitoses in the A1 region, but not in the A2, P1 or P2 regions, at 5 hours of *rpr* induction (Fig. 5B,C). By contrast, when mitotic cells were counted following longer exposure or later after *rpr* induction, mitoses were found to be extended throughout the whole A compartment. After 10 hours of *rpr* induction, mitotic cells were also found in the more anterior domain (A2). The number of mitoses in the P compartment during short or long exposure to *rpr* did not increase, as compared with control discs (Fig. 5D,E). This suggests that the P compartment does not contribute to regeneration of the *ptc* domain. However, a slight decrease in the frequency of mitosis in P1 at 5 hours of exposure and in P2 at 10 hours of exposure suggests an accommodation effect of the P compartment (Garcia-Bellido et al., 1994).

Ablation of the *ptc* domain also causes removal of most of the *dpp* (the *Drosophila Tgfβ* homologue), which is expressed in response to Hh and forms a narrow A-compartment stripe abutting the A/P border (Basler and Struhl, 1994; Capdevila et al., 1994). As Dpp protein forms a gradient that can be sensed by disc cells to control patterning and growth (Rogulja and Irvine, 2005), the *ptc>rpr* system could affect the overall growth status of the wing disc. Thus, it could be that

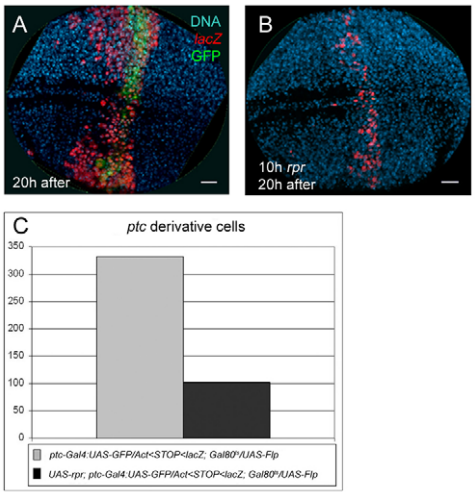

Fig. 4. Lineage tracing of the *ptc* domain. (**A**) Control wing disc in which the cell derivatives of the *ptc* domain (GFP, green) have populated an extensive area of the wing pouch (*lacZ*, red). (**B**) Disc in which *rpr* has been induced for 10 hours in the *ptc* domain and analysed 20 hours later. Note the reduction in the number of progeny (red). (**C**) The number of *lacZ*-positive cells derived from the *ptc* domain. Grey bar, control; black bar, *rpr* induced. The conditions for controls were exactly the same as the experimental except that these contained the *UAS-rpr* transgene. Scale bars: 15 μm.

regeneration is induced by Dpp from the re-established *dpp* domain, rather than by signals from the wound edges. Flies carrying the temperature-sensitive hh^{ts} allele were used to block *hh* expression and therefore minimise the capacity for reconstitution of the Dpp gradient. In these flies, *ptc>rpr* induction at 5 hours resulted in an increase in the number of mitoses in the A1 area, as occurs in normal regeneration (Fig. 5C). By contrast, at 10 hours of *ptc>rpr* induction, no increase was observed in the number of mitoses in the rest of the compartment (Fig. 5E). These data indicate that the later A-compartment-associated proliferation is driven by recovery of the Dpp morphogenetic gradient, whereas the early A1-associated mitoses are driven by a local Dpp-independent mechanism.

Mitosis in regenerating A-compartment tissue was associated with single cells or clusters of two to three synchronously dividing cells (see Fig. S3C in the supplementary material) with random orientations. Clusters of randomly dividing cells have been found in the normal developing wing pouch, albeit with up to ten mitotic cells per cluster (Milan et al., 1996). This difference in cluster size could indicate that in the regenerating A compartment, a high degree of asynchrony is accounted for by cells that are progressively recruited in order to recover the normal disc size in a short time (before molting and metamorphosis).

To test whether regenerative growth is associated with the damaged compartment, we analysed mitotic cells in *salm>rpr* discs, in which part of both the A and P compartments is removed. Under these conditions, mitotic cells were present in the regenerating apical epithelium of both the A and P compartments (Fig. 5F).

The JNK pathway in genetically induced regeneration

Expression of *puckered* (*puc*), a downstream effector of JNK, was analysed in *rpr*-induced discs using a *lacZ* reporter line to enable visualisation of cells that respond to high JNK activity. Five hours of induction resulted in *puc* localisation in a few cells close to the

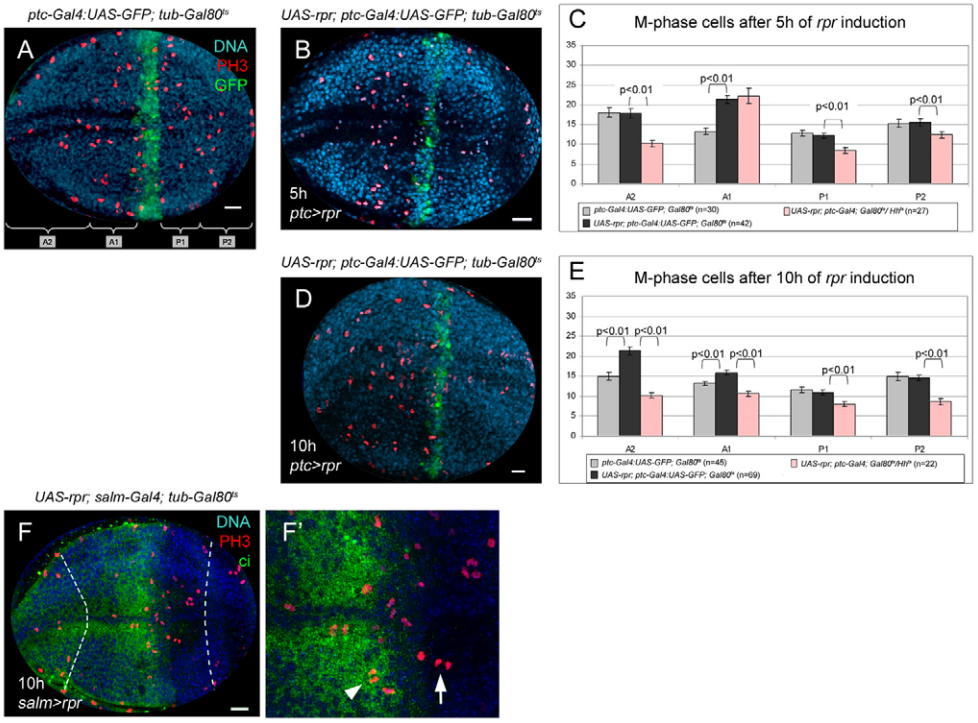

Fig. 5. Mitosis in cell death-induced discs. (**A**) Control disc illustrating the domains under consideration in the A and P compartments: A1 and P1 next to the wound and A2 and P2 far from the wound. (**B-E**) Confocal images of discs stained for anti-phospho-Histone H3 (PH3, red), *ptc*>GFP (green) and nuclei (blue) to show cells in M phase. Bar charts show the average number of dividing cells after *rpr* induction. Significant *P*-values are shown ($P<0.01$). (B,C) Mitosis after 5 hours of *rpr* induction. Note the increased number of dividing cells in A1 (B and black bars), even in the absence of Hh signal (pink bars). (D,E) Mitosis after 10 hours of *rpr* induction. Note that the increased proliferation has extended to the whole A compartment (A1 and A2 regions), whereas in the absence of Hh signalling proliferation has decreased in all domains. (**F**) Distribution of mitoses in a *salm>rpr* disc induced for 10 hours. This confocal image corresponds to the apical side, where most mitotic cells are concentrated in the regenerated tissue. Dashed lines indicate the limits of the ablated *salm* domain (compare with Fig. 3D). Green channel corresponds to Ci staining, which is specific for the A compartment. (**F′**) High-magnification view of the DV boundary in F. Arrow, posterior mitosis; arrowhead, anterior mitosis. In all images, anterior is to the left and posterior to the right. Scale bars: 15 μm.

wound, especially in DV boundary cells, in which closure is initiated (Fig. 6A). At this time point, the cells expressing the highest levels of *puc-lacZ* were located at the P-compartment edge, as revealed by the lack of co-staining with the anterior marker Ptc (Fig. 6B) or Ci (not shown). Nevertheless, weaker *puc* expression was also visible in a few A-compartment cells at this time (Fig. 6C). Ten hours of induction resulted in even more extensive *puc* expression, in a stripe of cells along the A/P boundary (Fig. 6D). These cells belonged to both A and P compartments, as confirmed by Ci and En co-staining (Fig. 6E,F). Five hours after induction, when healing is complete, the stripe of *puc*-positive cells was broader (Fig. 6G), with some of the highest levels of expression found in cells at the edge of the A compartment (Fig. 6H).

To determine the extent to which the JNK pathway is required for early regeneration induced by cell death, we used *hemipterous* (*hep*) hypomorphic alleles of the JNK kinase. Flies carrying transheterozygotic *hep* alleles and *ptc-Gal4/tub-Gal80^{ts}; UAS-rpr* were temperature shifted and regeneration analysed. We found disruption of the F-actin cable at P- and A-compartment edges (Fig. 7A). This alteration in cytoskeletal organisation was accompanied by a disruption of the healing edges. Indeed, the sharp interface between the intact epithelium and the dead cells found in normal discs was perturbed, as dead and living cells were found intermingled (Fig. 7A-C). Moreover, F-actin-rich cell extensions were absent on both sides of the wound, and in 60% of the discs the epithelium remained open and eventually degenerated. In the remaining 40% of the discs, partial healing occurred but did not follow the normal progression (from the DV border proximally and from apical to basal); instead, the wound was partially closed in some segments along the cell death domain and segments of apical epithelium remained open (Fig. 7B,C).

We also examined the effects of *hep* on proliferation. *hep* discs without *rpr* induction showed a slight decrease in the number of mitoses in A and P compartments when compared with wild type (Fig. 7E), but 5 hours of *rpr* induction increased the number of mitoses in the A1 domain. This suggests that at this time, the *hep* tissue can still respond by localising mitoses near the wound (Fig. 7D,E). Notably, however, local mitoses were only observed in discs that partially healed (n=6 out of 22), whereas completely unhealed *hep* discs did not exhibit any localised increase in mitosis (n=16 out of 22).

To confirm that regeneration was inhibited in a *hep*-heterozygous background, we analysed adult phenotypes after *rpr* induction. The *ptc-Gal4 UAS-rpr hep^{r75}* heterozygotes did not hatch, possibly owing to the effect of unhealed domains in different parts of the larvae, as *ptc* is also expressed outside the wing. Therefore, we used the *spalt^{PE}-Gal4* driver (see Fig. S2C,D in the supplementary material), which induces expression under a wing-specific enhancer of the *sal* promoter (Barrio and de Celis, 2004), to enable scoring of adult wings. In the absence of *rpr* induction, heterozygous *hep^{r75}* larvae developed normal wings. By contrast, 5 and 10 hours of *rpr* induction in *hep^{r75}*

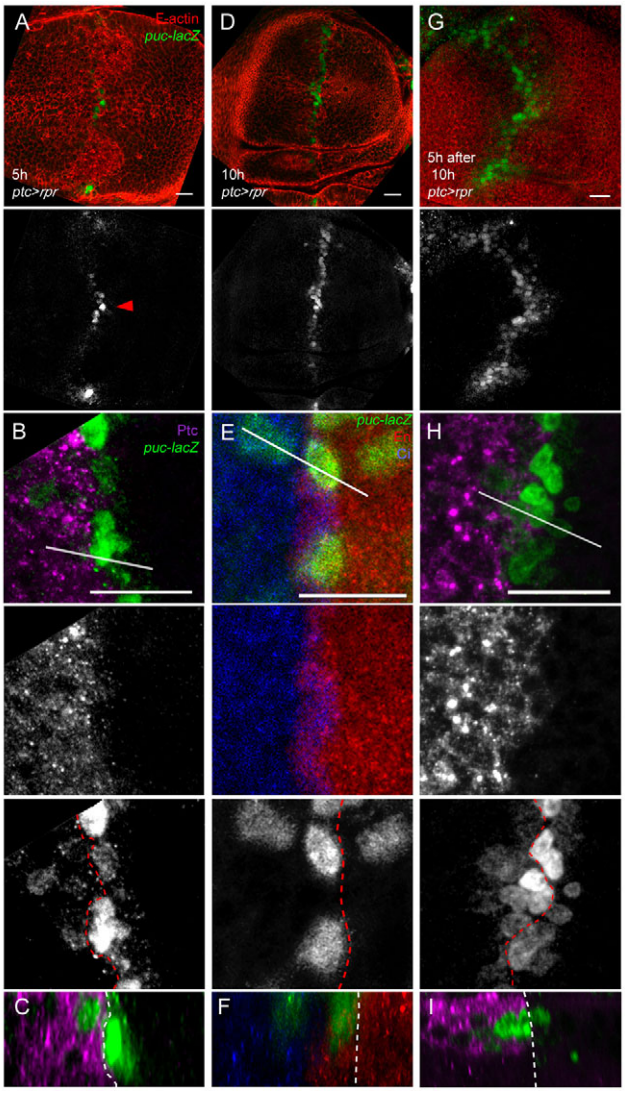

Fig. 6. *puc* expression after cell death-induced regeneration. (**A-C**) *rpr* induction for 5 hours. (A) Most of the first *puc-lacZ* cells (green or white) are concentrated close to the DV boundary (arrowhead). (B) *puc-lacZ* cells (green) are mainly posterior, as they lack expression of the anterior marker Ptc (purple). (C) Transverse section through the diagonal plane indicated in B. Note that an anterior cell is already expressing *puc-lacZ*. (**D-F**) *rpr* induction for 10 hours. *puc-lacZ* increases along the wound edges (D). At this time, Ci (blue) and En (red) co-staining shows that *puc-lacZ*-expressing cells are both anterior and posterior (E). Note that in third instar larva, a stripe of anterior cells abutting the A/P boundary expresses En (pink). (F) Transverse section through the plane indicated by the white line in E. (**G-I**) *rpr* induction for 10 hours observed 5 hours later. (H) The broadened *puc-lacZ* stripe consists of A- and P-compartment cells. (I) Transverse section through the plane indicated by the white line in H. Some of the *puc-lacZ* highly expressing cells are anterior at this time. In all images, anterior is to the left and posterior to the right. Dashed lines indicate the A/P boundary. Scale bars: 15 μm.

heterozygotes resulted in small wings in which part of the A and P compartments was missing (Fig. 7F). Thus, the ablated *sal* domain did not regenerate a complete wing in the hep^{r75}-sensitised background.

Different roles have been assigned to JNK in flies. Induction of apoptosis by X-ray irradiation generates an overall increase in JNK activity associated with apoptotic cells and results in compensatory proliferation of the neighbouring tissue (Perez-Garijo et al., 2009; Ryoo et al., 2004). Also, JNK becomes active in epithelial fusion processes that include cell shape changes and cytoskeletal reorganisation (Jacinto et al., 2002a; Martin and Wood, 2002). Thus, the stripe of *puc*-expressing cells could correspond to cells that will die or, alternatively, to cells that are active in the leading edges of the wound. To distinguish these two possibilities, we first examined whether the *puc* stripe corresponded to dying cells. Optical sections of TUNEL staining in *rpr*-induced *puc-lacZ*-tagged discs showed a clear localisation of *puc*-expressing cells in the apical epithelium and an absence of TUNEL incorporation in these cells; instead, as for Caspase-3, TUNEL localised to the basal zone of extruded cells (Fig. 8A). Even in basal *puc-lacZ* nuclei in the reconstituted epithelium, no colocalisation with markers of apoptosis could be found (Fig. 8B).

It might be that the JNK activity is below the detection level of *puc-lacZ* in dead cells. To address this possibility, we blocked JNK signalling within the dying domain using either *UAS-*bsk^{DN}, which targets the *basket* JNK kinase, or *UAS-puc*, which inhibits JNK activity. Using these transgenes activated in the *ptc* domain concomitantly with *rpr*, we found that wound healing and regeneration proceeded normally. Moreover, we found local mitosis in A1 at 5 hours of induction and mitoses further away in the A compartment at 10 hours of induction, at similar rates to those seen in discs with no inhibition of JNK signalling (Fig. 8D-G; see Fig. S4 in the supplementary material). Thus, perturbation of JNK signalling in living tissue results in severe defects in healing and proliferation but no such effect is seen following perturbation of JNK signalling in the dying domain. This suggests that JNK is required for cell death-induced healing and early regeneration, as observed following microsurgical fragmentation of imaginal discs (Bosch et al., 2005; Lee et al., 2005; Mattila et al., 2005).

DISCUSSION

Two main conclusions can be drawn from this work: (1) that genetically induced regeneration entails compartment-specific proliferation; and (2), that this type of regeneration requires JNK signalling for early regeneration events.

We have established that the proliferation response to *ptc>rpr* induction is concentrated in the A compartment and consists of two activities: a local and a compartment-associated response. The local proliferation response resembles the activity of blastemas, a feature found in discs after fragmentation and implantation (Abbott et al., 1981; Bosch et al., 2008; Bryant and Fraser, 1988; Fain and Alvarez, 1987; Karpen and Schubiger, 1981; O'Brochta and Bryant, 1987). The late compartment-restricted proliferation could be indicative of a reutilisation of developmental programmes. The entire A compartment responds to the lack of the original *ptc* region by reactivating proliferation in order to achieve the final organ size. Thus, we conclude that genetically induced regenerating discs restore the overall organ size by activation of proliferation, not only near the wound, as in fragmented and implanted discs, but also in the whole affected compartment. Thus, we believe that the local proliferation is a fast and early response to the lost structures and that the later compartment-associated proliferation is a response to adjust the size of the tissue.

We selected *ptc* and *sal* because of the precise removal of cells and also because they enabled us to test whether both A and P compartments are involved in regeneration. Our results suggest that when the A compartment is damaged (*ptc>rpr*), the P compartment only responds to the injury by sealing the gap that separates it from the A compartment through the generation of F-actin-rich cell

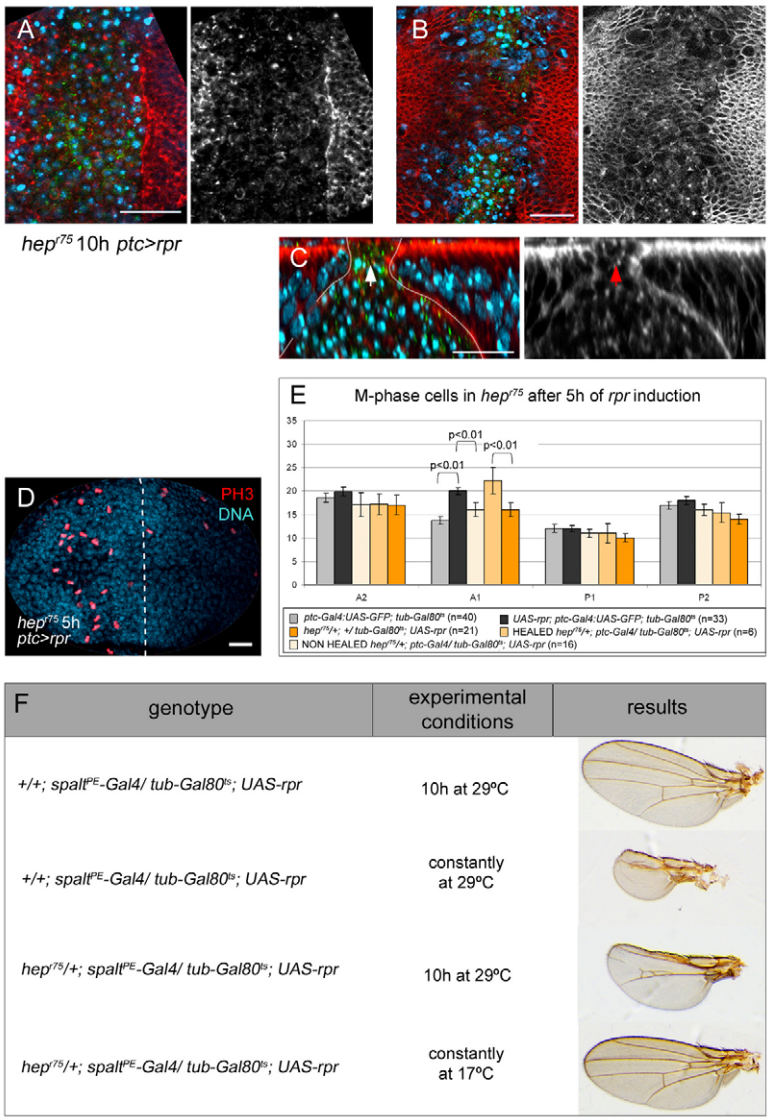

Fig. 7. The JNK pathway is necessary for regeneration after the induction of cell death. (**A-C**) Left panels show *hep*^{r75} discs after 10 hours of *rpr* induction (red, F-actin; green, Caspase-3; blue, nuclei); right panels show only the red channel. (A) *hep*^{r75} hypomorphic allele showing disrupted F-actin cable in the P compartment and even the absence of an F-actin cable at the A-compartment edge. (B) Apical view of *hep*^{r75} with incomplete wound repair. (C) Cross-section through an opened wound of the *hep*^{r75} disc. Arrow points to apical opening. The white line separates the dead from the regenerating domain. (**D**) *hep*^{r75} discs labelled with anti-PH3 showing a high concentration of mitoses near the wound of a 5 hour *rpr*-induced disc (red, anti-PH3; blue, nuclei). Dashed line indicates the A/P boundary. (**E**) Average numbers of mitoses in *hep*^{r75} and controls after 5 hours of *rpr* induction. *hep*^{r75} discs have been grouped into healed and unhealed discs. Note that healed discs show an increase in mitosis in A1 (see Fig. 5 for description of regions), as in wild type, whereas unhealed discs do not show an increase. Significant *P*-values are shown. (**F**) Wings after *rpr* induction with the *spalt*^{PE} promoter in the presence or absence of a *hep*^{r75} background. In the absence of the *hep*^{r75} allele, normal wings regenerate after 10 hours of *rpr* induction (top row), but do not regenerate when exposed to continuous *rpr* induction (second row). By contrast, in a *hep*^{r75} background, wings do not regenerate when exposed to *rpr* for 10 hours (third row). *hep*^{r75} wings develop normally at 17°C, at which temperature *rpr* is inactive (bottom row). Scale bars: 15 μm.

extensions. These are projected to anchor the extensions from the cells at the edge of the A compartment as they proceed towards recovery of the intact cell sheet. In this situation, the regenerated tissue is derived exclusively from the A compartment. By contrast, when cells from both the A and P compartments are killed (*sal>rpr*), proliferation increases in both compartments. The boundaries between compartments are rapidly re-established after injury and prevent cells from crossing into adjacent compartments (Abbott et al., 1981; Szabad et al., 1979). Thus, boundaries are respected and compartments act as units of growth during regeneration.

Following genetic ablation driven by either the *ptc* or *sal* drivers, healing starts at the DV boundary and spreads laterally towards the proximal regions, which are the last to close the wound. Cells at the DV boundary are arrested in G1–S, through a mechanism based on *Notch* and *wg* signalling (Herranz et al., 2008). These arrested cells are the first to respond to healing and drive the cytoskeletal machinery for tissue reorganisation. This is consistent with the idea that the requirements for cell proliferation and for cell shape changes that occur during normal fly and vertebrate development and wound repair place incompatible demands on the cytoskeletal machinery of the cell (Martin and Parkhurst, 2004). Another issue to be considered is that the DV boundary is the first zone of closure for F-actin extensions. This is reminiscent of *Drosophila* embryonic dorsal closure and wound repair, in which matching filopodia on both sides of the opening are recognised by the code of segment polarity genes in each parasegment (Jacinto et al., 2002b). In addition, mechanical forces may be involved in tissue reorganisation (Aegerter-Wilmsen et al., 2007; Hufnagel et al., 2007; Shraiman, 2005). Stretching forces could be altered upon the induction of cell death, and they could have an important role in mounting a quick healing response. For example, mechanical forces, which have been proposed to act in the developing wing disc and compress the tissue through the central region (Aegerter-Wilmsen et al., 2007), could stretch it towards the DV border after ablation of the *ptc* domain. Thus, either by matching affinities or by stretching forces, wound repair spreads from the apical DV border to basal and proximal domains.

It has been shown in the *Drosophila* wing disc that massive loss of cells after irradiation gives rise to apparently normal adult wings as a result of compensatory proliferation driven by surviving cells (Haynie and Bryant, 1977; James and Bryant, 1981). Experiments involving irradiation or induction of apoptosis in a p35 background have suggested that this compensatory proliferation is controlled by signals, including JNK, emerging from cells that have entered apoptosis (Huh et al., 2004; Perez-Garijo et al., 2004; Perez-Garijo

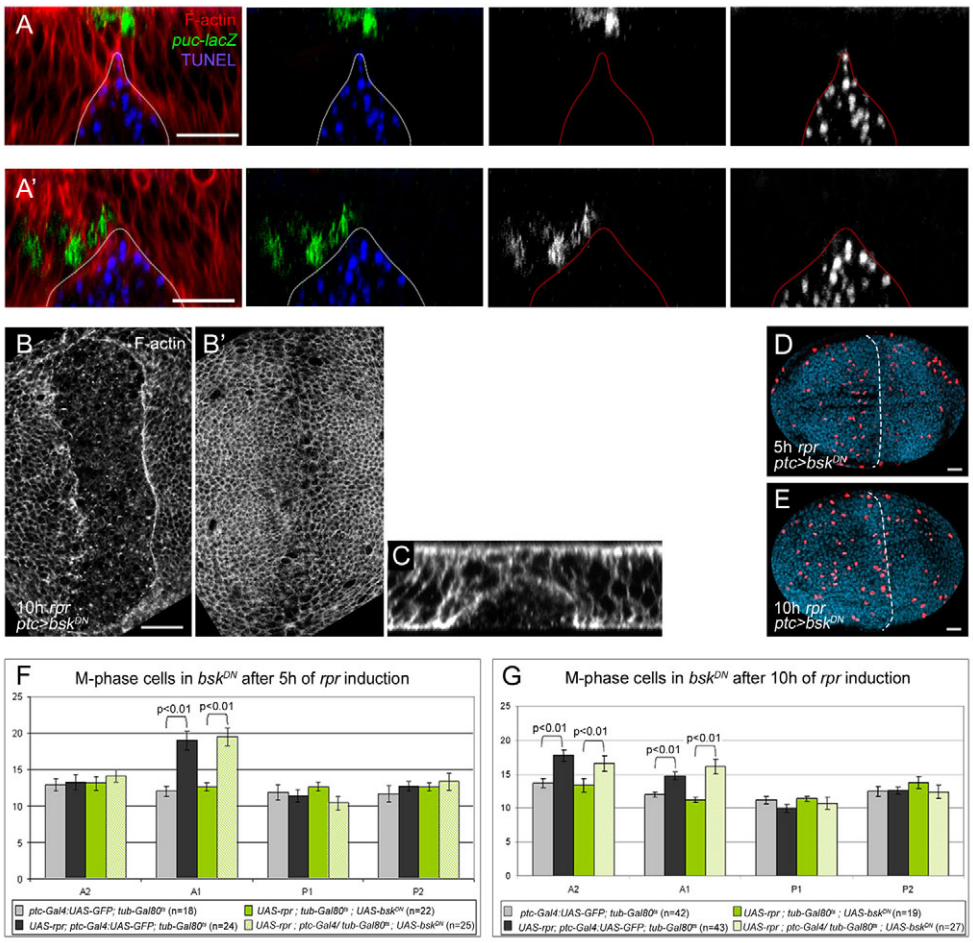

Fig. 8. JNK is not required in the dead domain for regeneration. (**A**,**A′**) Transverse sections of *rpr*-induced discs showing *puc-lacZ* cells (green) and basal TUNEL incorporation in apoptotic cells (blue); F-actin is red. Normally, *puc-lacZ* cells are apical (A). Note that in A′, the *puc-lacZ* nuclei are close to apoptotic cells, but did not incorporate TUNEL. The lines (white or red) indicate the separation of the basal extruding apoptotic cells (below) from the living regenerating tissue (above). (**B-C**) Regenerative response of *rpr*-induced disc expressing a dominant-negative form of Basket (Bsk) in the death domain (*ptc*). (B,C) F-actin labelling showing normal healing. Basal (B), apical (B′) and transverse section (C) of a disc with *rpr* induced for 10 hours. Note that neither the actin cable (B) nor apical closure (B′,C) is affected when JNK is specifically blocked in dying cells. (**D-G**) Distribution of mitoses after *rpr* induction. No changes in A1 first (D,F) or A1 and A2 later (E,G) were found after coactivation of bsk^{DN} (see Fig. 5 for description of domains). In all images, anterior is to the left and posterior to the right. Scale bars: 15 μm.

et al., 2005; Ryoo et al., 2004), and that cell-death regulators, such as p53 and the caspase Dronc (Nedd2-like caspase – FlyBase), function as regulators of compensatory proliferation and blastema formation in the surviving cells (Kondo et al., 2006; Wells et al., 2006). By contrast, our results show that proliferation is compartment specific and occurs independently of the dead tissue following targeted ablation. Two observations strongly support this interpretation. First, *puc* expression, as a marker of JNK activity, is concentrated in a narrow strip of apical cells (Fig. 6), suggesting that JNK signalling is activated in the leading edges during wound closure. This again resembles other repair mechanisms described not only in imaginal discs, but also in other healing tissues, and reiterates epithelial fusion events observed in embryogenesis (Martin and Parkhurst, 2004). Second, perturbation of the JNK pathway within the dying domain has no effect on either healing or regeneration (Fig. 8 and see Fig. S4 in the supplementary material). Even the early peak of localised mitosis near the wound and the later A-compartment-associated mitoses are present when *UAS-*bsk^{DN} and *UAS-puc* are driven in the dying domain. Effects on healing and regeneration are only found in *hep* mutant backgrounds, when JNK is impaired in the whole epithelium and not only in the dead domain. This requirement for the JNK pathway at the edges of the wound has also been found in studies of microsurgically induced regeneration (Bosch et al., 2005; Mattila et al., 2005). Cell lineage analysis of *puc*-expressing cells near the wound has shown that *puc* sets the limits of a blastema and that *puc* derivatives are able to reconstitute most of the missing tissue (Bosch et al., 2008).

Finally, whether JNK is required for healing alone or also functions as a signal for proliferation remains an open issue. We have shown that rapid local proliferation is affected in unhealed *hep* heterozygotes. Also, sal^{PE}>*rpr* wing regeneration cannot be achieved after 10 hours induction in a hep^{r75} background. Reduced proliferation could be due to a lack of healing or to loss of JNK activity. We cannot rule out the possibility that the JNK cascade, through the active AP-1 (Kayak and Jun-related antigen – FlyBase) transcription factor complex, targets not only genes required for healing and epithelial fusion, but also those required for regenerative growth. In mammals, inhibition of the JNK pathway or lack of c-Jun results in eyelid-closure defects and also impairs proliferation by targeting *Egfr* transcription (Zenz et al., 2003; Weston et al., 2004). Reconstruction of normal pattern and size might also require multiple signals. It has recently been found that regenerative growth induced by cell death requires Wnt/Wg signalling to increase dMyc stability (Smith-Bolton et al., 2009), suggesting the involvement of other signalling pathways and also cell competition (de la Cova et al., 2004; Moreno and Basler, 2004; Moreno et al., 2002; Ninov et al., 2007). It is very likely that an integrated network of signals and cell behaviours is necessary to reconstitute the damaged tissue.

Taken together, our results suggest a model for cell-induced regeneration that includes two phases. The first, which occurs near the wound edges, involves JNK activity and is important for healing and rapid local proliferation. The second involves proliferation to compensate for the lost tissue and is extended throughout the

damaged compartment. As in normal development, the regenerative growth that occurs in this second phase requires the reconstitution of morphogenetic signals that drive proliferation.

Acknowledgements
We thank the following colleagues for helpful discussions, suggestions and encouragement throughout this study: Jaume Baguñà, Enrique Martín-Blanco, Marco Milán, Ginés Morata, Eduardo Moreno and Gerold Schubiger. We thank the confocal facility of the Serveis Científico-Tècnics at the University of Barcelona for help with microscopy. This work was supported by the Consolider-Ingenio 2010 Program (CSD2007-00008) and a grant (BFU2006-07334/BMC) from the Spanish Ministerio de Ciencia y Tecnología. C.B. was supported by a fellowship from the Spanish Ministerio de Ciencia y Tecnología.

Competing interests statement
The authors declare no competing financial interests.

Supplementary material
Supplementary material for this article is available at
http://dev.biologists.org/lookup/suppl/doi:10.1242/dev.045559/-/DC1

References
Abbott, L. C., Karpen, G. H. and Schubiger, G. (1981). Compartmental restrictions and blastema formation during pattern regulation in Drosophila imaginal leg discs. *Dev. Biol.* **87**, 64-75.
Adler, P. N. (1981). Growth during pattern regulation in imaginal discs. *Dev. Biol.* **87**, 356-373.
Aegerter-Wilmsen, T., Aegerter, C. M., Hafen, E. and Basler, K. (2007). Model for the regulation of size in the wing imaginal disc of Drosophila. *Mech. Dev.* **124**, 318-326.
Agata, K., Saito, Y. and Nakajima, E. (2007). Unifying principles of regeneration I: Epimorphosis versus morphallaxis. *Dev. Growth Differ.* **49**, 73-78.
Agnes, F., Suzanne, M. and Noselli, S. (1999). The Drosophila JNK pathway controls the morphogenesis of imaginal discs during metamorphosis. *Development* **126**, 5453-5462.
Ashburner, M., Golic, K. and Hawley, R. (2005). *Drosophila: A Laboratory Handbook*. New York: Cold Spring Harbor Laboratory Press.
Barrio, R. and de Celis, J. F. (2004). Regulation of spalt expression in the *Drosophila* wing blade in response to the Decapentaplegic signaling pathway. *Proc. Natl. Acad. Sci. USA* **101**, 6021-6026.
Basler, K. and Struhl, G. (1994). Compartment boundaries and the control of Drosophila limb pattern by hedgehog protein. *Nature* **368**, 208-214.
Bodenstein, D. (1943). Hormones and tissue competence in the development of Drosophila. *Biol. Bull.* **84**, 34-58.
Bosch, M., Serras, F., Martin-Blanco, E. and Baguna, J. (2005). JNK signaling pathway required for wound healing in regenerating Drosophila wing imaginal discs. *Dev. Biol.* **280**, 73-86.
Bosch, M., Baguna, J. and Serras, F. (2008). Origin and proliferation of blastema cells during regeneration of Drosophila wing imaginal discs. *Int. J. Dev. Biol.* **52**, 1043-1050.
Brand, A. H. and Perrimon, N. (1993). Targeted gene expression as a means of altering cell fates and generating dominant phenotypes. *Development* **118**, 401-415.
Brockes, J. P. and Kumar, A. (2008). Comparative aspects of animal regeneration. *Annu. Rev. Cell Dev. Biol.* **24**, 525-549.
Brook, W. J., Ostafichuk, L. M., Piorecky, J., Wilkinson, M. D., Hodgetts, D. J. and Russell, M. A. (1993). Gene expression during imaginal disc regeneration detected using enhancer-sensitive P-elements. *Development* **117**, 1287-1297.
Bryant, P. J. (1971). Regeneration and duplication following operations in situ on the imaginal discs of Drosophila melanogaster. *Dev. Biol.* **26**, 637-651.
Bryant, P. J. and Fraser, S. E. (1988). Wound healing, cell communication, and DNA synthesis during imaginal disc regeneration in Drosophila. *Dev. Biol.* **127**, 197-208.
Capdevila, J., Estrada, M. P., Sanchez-Herrero, E. and Guerrero, I. (1994). The Drosophila segment polarity gene patched interacts with decapentaplegic in wing development. *EMBO J.* **13**, 71-82.
Chera, S., Ghila, L., Dobretz, K., Wenger, Y., Bauer, C., Buzgariu, W., Martinou, J. C. and Galliot, B. (2009). Apoptotic cells provide an unexpected source of Wnt3 signaling to drive hydra head regeneration. *Dev. Cell* **17**, 279-289.
de la Cova, C., Abril, M., Bellosta, P., Gallant, P. and Johnston, L. A. (2004). Drosophila myc regulates organ size by inducing cell competition. *Cell* **117**, 107-116.
Dunne, J. F. (1981). Growth dynamics in the regeneration of a fragment of the wing imaginal disc of Drosophila melanogaster. *Dev. Biol.* **87**, 379-382.
Fain, M. J. and Alvarez, C. (1987). The cell cycle and its relation to growth during pattern regulation in wing discs of Drosophila. *J. Insect Physiol.* **33**, 697-705.
Fan, Y. and Bergmann, A. (2008). Distinct mechanisms of apoptosis-induced compensatory proliferation in proliferating and differentiating tissues in the Drosophila eye. *Dev. Cell* **14**, 399-410.
Galliot, B., Tanaka, E. and Simon, A. (2008). Regeneration and tissue repair: themes and variations. *Cell Mol. Life Sci.* **65**, 3-7.
Garcia-Bellido, A. and Merriam, J. R. (1971). Parameters of the wing imaginal disc development of Drosophila melanogaster. *Dev. Biol.* **24**, 61-87.
Garcia-Bellido, A., Cortes, F. and Milan, M. (1994). Cell interactions in the control of size in Drosophila wings. *Proc. Natl. Acad. Sci. USA* **91**, 10222-10226.
Glise, B., Bourbon, H. and Noselli, S. (1995). hemipterous encodes a novel Drosophila MAP kinase kinase, required for epithelial cell sheet movement. *Cell* **83**, 451-461.
Hadorn, E. (1963). Differenzierungsleistungen wiederholt fragmentierter Teilstücke männlicher Genitalscheiben von Drosophila melanogaster nach Kultur in vivo. *Dev. Biol.* **7**, 617-629.
Hadorn, E., Hürlimann, R., Mindek, G., Schubiger, G. and Staub, M. (1968). Developmental capacity of embryonal blastema in Drosophila following cultivation in an adult host. *Rev. Suisse Zool.* **75**, 557-569.
Handberg-Thorsager, M., Fernandez, E. and Salo, E. (2008). Stem cells and regeneration in planarians. *Front. Biosci.* **13**, 6374-6394.
Hay, B. A., Wolff, T. and Rubin, G. M. (1994). Expression of baculovirus P35 prevents cell death in Drosophila. *Development* **120**, 2121-2129.
Haynie, J. and Bryant, P. J. (1977). The effects of X-rays on the proliferation dynamics of cells in the imaginal wing disc of Drosophila melanogaster *Roux's Arch. Dev. Biol.* **183**, 85-100.
Herranz, H., Perez, L., Martin, F. A. and Milan, M. (2008). A Wingless and Notch double-repression mechanism regulates G1-S transition in the Drosophila wing. *EMBO J.* **27**, 1633-1645.
Hinz, U., Giebel, B. and Campos-Ortega, J. A. (1994). The basic-helix-loop-helix domain of Drosophila lethal of scute protein is sufficient for proneural function and activates neurogenic genes. *Cell* **76**, 77-87.
Hufnagel, L., Teleman, A. A., Rouault, H., Cohen, S. M. and Shraiman, B. I. (2007). On the mechanism of wing size determination in fly development. *Proc. Natl. Acad. Sci. USA* **104**, 3835-3840.
Huh, J. R., Guo, M. and Hay, B. A. (2004). Compensatory proliferation induced by cell death in the Drosophila wing disc requires activity of the apical cell death caspase Dronc in a nonapoptotic role. *Curr. Biol.* **14**, 1262-1266.
Jacinto, A., Wood, W., Woolner, S., Hiley, C., Turner, L., Wilson, C., Martinez-Arias, A. and Martin, P. (2002a). Dynamic analysis of actin cable function during Drosophila dorsal closure. *Curr. Biol.* **12**, 1245-1250.
Jacinto, A., Woolner, S. and Martin, P. (2002b). Dynamic analysis of dorsal closure in Drosophila: from genetics to cell biology. *Dev. Cell* **3**, 9-19.
James, A. A. and Bryant, P. J. (1981). A quantitative study of cell death and mitotic inhibition in gamma-irradiated imaginal wing discs of Drosophila melanogaster. *Radiat. Res.* **87**, 552-564.
Jasper, H., Benes, V., Schwager, C., Sauer, S., Clauder-Munster, S., Ansorge, W. and Bohmann, D. (2001). The genomic response of the Drosophila embryo to JNK signaling. *Dev. Cell* **1**, 579-586.
Karpen, G. H. and Schubiger, G. (1981). Extensive regulatory capabilities of a Drosophila imaginal disk blastema. *Nature* **294**, 744-747.
Kondo, S., Senoo-Matsuda, N., Hiromi, Y. and Miura, M. (2006). DRONC coordinates cell death and compensatory proliferation. *Mol. Cell. Biol.* **26**, 7258-7268.
Kragl, M., Knapp, D., Nacu, E., Khattak, S., Maden, M., Epperlein, H. H. and Tanaka, E. M. (2009). Cells keep a memory of their tissue origin during axolotl limb regeneration. *Nature* **460**, 60-65.
Lee, N., Maurange, C., Ringrose, L. and Paro, R. (2005). Suppression of Polycomb group proteins by JNK signalling induces transdetermination in Drosophila imaginal discs. *Nature* **438**, 234-237.
Lepilina, A., Coon, A. N., Kikuchi, K., Holdway, J. E., Roberts, R. W., Burns, C. G. and Poss, K. D. (2006). A dynamic epicardial injury response supports progenitor cell activity during zebrafish heart regeneration. *Cell* **127**, 607-619.
Li, W. and Baker, N. E. (2007). Engulfment is required for cell competition. *Cell* **129**, 1215-1225.
Ma, C., Zhou, Y., Beachy, P. A. and Moses, K. (1993). The segment polarity gene hedgehog is required for progression of the morphogenetic furrow in the developing Drosophila eye. *Cell* **75**, 927-938.
Martin, P. and Wood, W. (2002). Epithelial fusions in the embryo. *Curr. Opin. Cell Biol.* **14**, 569-574.
Martin, P. and Parkhurst, S. M. (2004). Parallels between tissue repair and embryo morphogenesis. *Development* **131**, 3021-3034.
Martin-Blanco, E., Gampel, A., Ring, J., Virdee, K., Kirov, N., Tolkovsky, A. M. and Martinez-Arias, A. (1998). Puckered encodes a phosphatase that mediates a feedback loop regulating JNK activity during dorsal closure in Drosophila. *Genes Dev.* **12**, 557-570.
Mattila, J., Omelyanchuk, L., Kyttala, S., Turunen, H. and Nokkala, S. (2005). Role of Jun N-terminal Kinase (JNK) signaling in the wound healing and regeneration of a Drosophila melanogaster wing imaginal disc. *Int. J. Dev. Biol.* **49**, 391-399.

McGuire, S. E., Le P. T., Osborn, A. J., Matsumoto, K. and Davis, R. L. (2003). Spatiotemporal rescue of memory dysfunction in Drosophila. *Science* **302**, 1765-1768.
Milan, M., Campuzano, S. and Garcia-Bellido, A. (1996). Cell cycling and patterned cell proliferation in the wing primordium of Drosophila. *Proc. Natl. Acad. Sci. USA* **93**, 640-645.
Millard, T. H. and Martin, P. (2008). Dynamic analysis of filopodial interactions during the zippering phase of Drosophila dorsal closure. *Development* **135**, 621-626.
Moreno, E. and Basler, K. (2004). dMyc transforms cells into super-competitors. *Cell* **117**, 117-129.
Moreno, E., Basler, K. and Morata, G. (2002). Cells compete for decapentaplegic survival factor to prevent apoptosis in Drosophila wing development. *Nature* **416**, 755-759.
Morgan, T. H. (1901). Regeneration and Liability to Injury. *Science* **14**, 235-248.
Motzny, C. K. and Holmgren, R. (1995). The *Drosophila* cubitus interruptus protein and its role in the wingless and hedgehog signal transduction pathways. *Mech. Dev.* **52**, 137-150.
Ninov, N., Chiarelli, D. A. and Martin-Blanco, E. (2007). Extrinsic and intrinsic mechanisms directing epithelial cell sheet replacement during Drosophila metamorphosis. *Development* **134**, 367-379.
O'Brochta, D. A. and Bryant, P. J. (1987). Distribution of S-phase cells during the regeneration of Drosophila imaginal wing discs. *Dev. Biol.* **119**, 137-142.
Perez-Garijo, A., Martin, F. A. and Morata, G. (2004). Caspase inhibition during apoptosis causes abnormal signalling and developmental aberrations in Drosophila. *Development* **131**, 5591-5598.
Perez-Garijo, A., Martin, F. A., Struhl, G. and Morata, G. (2005). Dpp signaling and the induction of neoplastic tumors by caspase-inhibited apoptotic cells in Drosophila. *Proc. Natl. Acad. Sci. USA* **102**, 17664-17669.
Perez-Garijo, A., Shlevkov, E. and Morata, G. (2009). The role of Dpp and Wg in compensatory proliferation and in the formation of hyperplastic overgrowths caused by apoptotic cells in the Drosophila wing disc. *Development* **136**, 1169-1177.
Poss, K. D. (2007). Getting to the heart of regeneration in zebrafish. *Semin. Cell Dev. Biol.* **18**, 36-45.
Ramet, M., Lanot, R., Zachary, D. and Manfruelli, P. (2002). JNK signaling pathway is required for efficient wound healing in Drosophila. *Dev. Biol.* **241**, 145-156.
Reinhardt, C. A. and Bryant, P. J. (1981). Wound healing in the imaginal discs of Drosophila. II. Transmission electron microscopy of normal and healing wing discs. *J. Exp. Zool.* **216**, 45-61.
Reinhardt, C. A., Hodgkin, N. M. and Bryant, P. J. (1977). Wound healing in the imaginal discs of Drosophila. I. Scanning electron microscopy of normal and healing wing discs. *Dev. Biol.* **60**, 238-257.
Rogulja, D. and Irvine, K. D. (2005). Regulation of cell proliferation by a morphogen gradient. *Cell* **123**, 449-461.
Russell, M. A., Ostafichuk, L. and Scanga, S. (1998). Lethal P-lacZ insertion lines expressed during pattern respecification in the imaginal discs of Drosophila. *Genome* **41**, 7-13.
Ryoo, H. D., Gorenc, T. and Steller, H. (2004). Apoptotic cells can induce compensatory cell proliferation through the JNK and the Wingless signaling pathways. *Dev. Cell* **7**, 491-501.
Salmeron, J. M., Jr, Leuther, K. K. and Johnston, S. A. (1990). GAL4 mutations that separate the transcriptional activation and GAL80-interactive functions of the yeast GAL4 protein. *Genetics* **125**, 21-27.
Schubiger, G. (1971). Regeneration, duplication and transdetermination in fragments of the leg disc of Drosophila melanogaster. *Dev. Biol.* **26**, 277-295.
Shraiman, B. I. (2005). Mechanical feedback as a possible regulator of tissue growth. *Proc. Natl. Acad. Sci. USA* **102**, 3318-3323.
Slack, J. M., Lin, G. and Chen, Y. (2008). The Xenopus tadpole: a new model for regeneration research. *Cell Mol. Life Sci.* **65**, 54-63.
Smith-Bolton, R. K., Worley, M. I., Kanda, H. and Hariharan, I. K. (2009). Regenerative growth in Drosophila imaginal discs is regulated by Wingless and Myc. *Dev. Cell* **16**, 797-809.
Struhl, G. and Basler, K. (1993). Organizing activity of wingless protein in *Drosophila*. *Cell* **72**, 527-540.
Szabad, J., Simpson, P. and Nothiger, R. (1979). Regeneration and compartments in Drosophila. *J. Embryol. Exp. Morphol.* **49**, 229-241.
Weber, U., Paricio, N. and Mlodzik, M. (2000). Jun mediates Frizzled-induced R3/R4 cell fate distinction and planar polarity determination in the Drosophila eye. *Development* **127**, 3619-3629.
Wells, B. S., Yoshida, E. and Johnston, L. A. (2006). Compensatory proliferation in Drosophila imaginal discs requires Dronc-dependent p53 activity. *Curr. Biol.* **16**, 1606-1615.
Weston, C. R., Wong, A., Hall, J. P., Goad, M. E., Flavell, R. A. and Davis, R. J. (2004). The c-Jun NH2-terminal kinase is essential for epidermal growth factor expression during epidermal morphogenesis. *Proc. Natl. Acad. Sci. USA* **101**, 14114-14119.
Wing, J. P., Zhou, L., Schwartz, L. M. and Nambu, J. R. (1998). Distinct cell killing properties of the Drosophila reaper, head involution defective, and grim genes. *Cell Death Differ.* **5**, 930-939.
Wood, W., Jacinto, A., Grose, R., Woolner, S., Gale, J., Wilson, C. and Martin, P. (2002). Wound healing recapitulates morphogenesis in Drosophila embryos. *Nat. Cell Biol.* **4**, 907-912.
Yoo, S. J., Huh, J. R., Muro, I., Yu, H., Wang, L., Wang, S. L., Feldman, R. M., Clem, R. J., Muller, H. A. and Hay, B. A. (2002). Hid, Rpr and Grim negatively regulate DIAP1 levels through distinct mechanisms. *Nat. Cell Biol.* **4**, 416-424.
Zeidler, M. P., Tan, C., Bellaiche, Y., Cherry, S., Hader, S., Gayko, U. and Perrimon, N. (2004). Temperature-sensitive control of protein activity by conditionally splicing inteins. *Nat. Biotechnol.* **22**, 871-876.
Zeitlinger, J. and Bohmann, D. (1999). Thorax closure in Drosophila: involvement of Fos and the JNK pathway. *Development* **126**, 3947-3956.
Zenz, R., Scheuch, H., Martin, P., Frank, C., Eferl, R., Kenner, L., Sibilia, M. and Wagner, E. F. (2003). c-Jun regulates eyelid closure and skin tumor development through EGFR signaling. *Dev. Cell* **4**, 879-889.